

Gas-Phase Synthesis of Coronene through Stepwise Directed Ring Annulation

Shane J. Goettl¹, Lotefa B. Tuli², Andrew M. Turner¹, Yahaira Reyes², A. Hasan Howlader^{2†}, Stanislaw F. Wnuk², Patrick Hemberger^{*3}, Alexander M. Mebel^{*2}, Ralf I. Kaiser^{*1}

Affiliations

¹ *Department of Chemistry, University of Hawai‘i at Mānoa, Honolulu, HI 96822, USA*

² *Department of Chemistry and Biochemistry, Florida International University, Miami, FL 33199, USA*

³ *Paul Scherrer Institute, CH-5232, Villigen PSI, Switzerland*

[†] *Present address: Department of Chemistry, Johns Hopkins University, Baltimore, MD 21218, USA*

* Correspondance: ralfk@hawaii.edu, mebela@fiu.edu, patrick.hemberger@psi.ch

Table of Contents

1. Precursor Synthesis and Characterization

2. Mass Spectra Analysis

3. Test Reaction

4. Table S1 and Figures S1–S13

5. Supporting References

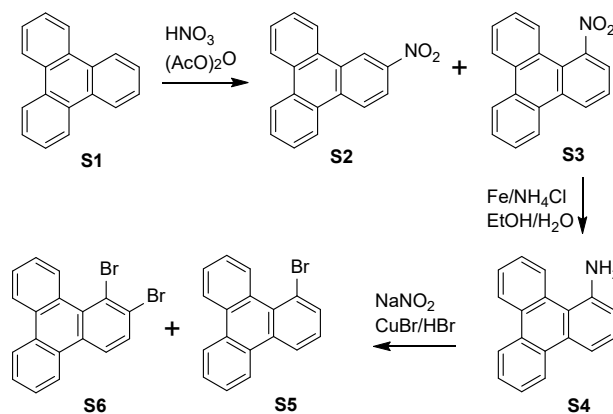
1. Precursor Synthesis and Characterization

1.1. General Information:

^1H NMR spectra at 400 MHz and ^{13}C NMR at 100.6 MHz were recorded on a Bruker 400 MHz instrument with solutions of CDCl_3 . All chemical shift values are reported in parts per million (ppm) and referenced to the residual solvent peaks of CDCl_3 (7.26 ppm) for ^1H NMR and the CDCl_3 (77.2 ppm) peaks for ^{13}C NMR spectra, with coupling constant (J) values reported in Hz. TLC was performed on Merck Kieselgel 60-F₂₅₄, and products were detected with 254 nm light. Merck Kieselgel 60 (230-400 mesh) was used for column chromatography. For ultrasonic vibration a Branson ultrasonic cleaner, Model 5200, was used. All reagents and solvents were purchased from commercial suppliers and dried using standard procedures. Anhydrous THF and triphenylene **S1** were purchased from Fisher Scientific and benzo[ghi]perylene **S7** was purchased from Ambeed Inc. and used without further purification.

1.2. Synthesis of 1-bromotriphenylene (S5):

1-Bromotriphenylene **S5** was synthesized by diazotization-bromination of 1-aminotriphenylene, which was prepared from commercially available triphenylene via nitration followed by reduction. Thus, nitration of triphenylene **S1** with $\text{HNO}_3/(\text{AcO})_2\text{O}$ gave a mixture of 2-nitrotriphenylene **S2** (20%) and 1-nitrotriphenylene **S3** (30%),¹ which were separated on silica gel column (Scheme 1). Reduction of **S3** with Fe powder/ NH_4Cl produced 1-aminotriphenylene **S4**. Subsequent, diazotization-bromination of **S4** with $\text{NaNO}_2/\text{CuBr}/\text{HBr}$ provided mixture of 1-bromotriphenylene **S5**/1,2-dibromotriphenylene **S6** (77:23).



Scheme 1. Synthesis of 1-bromotriphenylene **S5**.

2-Nitrotriphenylene (S2) and 1-Nitrotriphenylene (S3). The triphenylene **S1** (10.0 g, 43.8 mmol) was dissolved in Ac₂O (60 mL) in a flame-dried flask. HNO₃ (2.80 mL, 70% w/w) was added into the mixture dropwise for 10 minutes. The reaction mixture was stirred at 60 °C for 1 h. The reaction mixture was diluted with EtOAc (100 mL) and was extracted with H₂O (100 x 5). The organic layer was washed with saturated NaHCO₃ (50 mL x 5), brine (100 mL) and dried over anhydrous Na₂SO₄. Volatiles were evaporated and the residue was column chromatographed (5 → 20% EtOAc/hexane) to give **S3** (3.6 g, 30%) and **S2** (2.4 g, 20%) as light-yellow powder.¹ More polar compound **S3** had: ¹H NMR (CDCl₃) δ 7.51 (t, *J* = 7.8 Hz, 1H), 7.59–7.71 (m, 4H), 7.79 (d, *J* = 7.6 Hz, 1H), 8.00 (d, *J* = 8.4 Hz, 1H), 8.50 (d, *J* = 7.4 Hz, 1H), 8.57 (d, *J* = 7.6 Hz, 2H), 8.70 (d, *J* = 8.2 Hz, 1H); ¹³C NMR (CDCl₃) δ 122.44, 123.33, 123.50, 123.62, 127.78, 125.37, 126.33, 126.45, 126.54, 127.16, 127.97, 128.20, 128.66, 128.78, 130.40, 131.11, 132.50, 149.90. Less polar **S2** had: ¹H NMR (CDCl₃) δ 7.65–7.77 (m, 4H), 8.31 (dd, *J* = 8.8, 2.4 Hz, 1H), 8.51 – 8.62 (m, 5H), 9.35 (d, *J* = 2.4 Hz, 1H); ¹³C NMR (CDCl₃) δ 119.24, 120.99, 123.54, 123.65, 124.35, 124.57, 127.88, 128.02, 128.23, 128.69, 128.75, 129.28, 130.10, 130.24, 131.11, 134.44, 146.49.

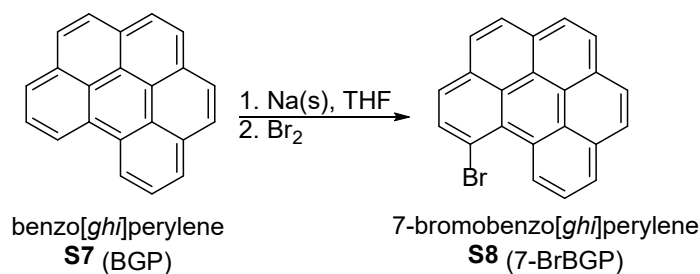
1-Aminotriphenylene (S4). Iron powder (4.38 g, 78.5 mmol) was added to the solution of NH₄Cl (4.2 g, 78.5 mmol) in H₂O/EtOH (60 mL, 1:1) in a flask equipped with a stir bar. The mixture was stirred at 60 °C for 30 min to activate the iron powder. Then, 1-nitrotriphenylene **S3** (742 mg, 3.0 mmol) was added and the temperature of reaction mixture was raised to 80 °C and stirring was continued for another 30 min. The mixture was cooled with ice bath, basified with dilute aqueous NaOH to pH ~12 and was filtered to remove solid residue. The filtrate was concentrated under reduced pressure and extracted with EtOAc. The organic layer was separated, dried over anhydrous Na₂SO₄, filtered, and evaporated. The residue was purified by column chromatography (20 → 30% EtOAc/hexane) to give **S4** (2.45 g, 83%) as a yellow solid: ¹H NMR (CDCl₃) δ 4.37 (s, 2H), 6.98 (d, *J* = 7.6 Hz, 1H), 7.43 (t, *J* = 8.0 Hz, 1H), 7.55–7.66 (m, 4H), 8.11 (d, *J* = 8.0 Hz, 1H), 8.55–8.67 (m, 3H), 9.22 (d, *J* = 7.9 Hz, 1H); ¹³C NMR (CDCl₃) δ 114.22, 115.99, 118.85, 123.13, 123.70, 123.99, 126.09, 126.32, 126.36, 127.31, 127.38, 130.12, 130.27, 130.42, 130.49, 132.22, 145.20.

1-Bromotriphenylene (S5) and 1,2-dibromotriphenylene (S6). The 1-Aminotriphenylene **S4** (200 mg, 0.82 mmol) was dissolved in mixture of MeCN/H₂O (16 mL, 1:1). Then, pre-cooled HBr (48%, 5 mL) was added and stirred at 0 °C. Aqueous solution of NaNO₂ (85 mg, 1.2 mmol; 1.0 mL) was added into the mixture dropwise for 2 minutes. The reaction mixture was stirred at 0 °C

for 20 min. Next, pre-cooled CuBr (128 mg, 0.9 mmol) solution in HBr (8 mL) solution was added at rt and stirred for 2 h. The reaction mixture was transferred into a separatory funnel and EtOAc (20 mL) was added, which was extracted with H₂O (10 mL x 5). The organic layer was washed with saturated NaHCO₃ (50 mL x 2), brine (50 mL) and dried over anhydrous Na₂SO₄. Volatiles were evaporated and the residue was column chromatographed (5 → 10% EtOAc/hexane) to give inseparable mixture of **S5** and 1,2-dibromotriphenylene **S6** (100 mg, 40%; 77:23) as off-white powder. ¹H NMR (400 MHz, CDCl₃) δ 7.40 (t, *J* = 8.0 Hz, 1H), 7.52 – 7.70 (m, 5.5H), 7.81 (d, *J* = 8.8 Hz, 0.3H), 7.94 (dd, *J* = 7.6, 1.2 Hz, 1H), 8.32 (dd, *J* = 8.8, 0.8 Hz, 0.3H), 8.39 – 8.42 (m, 0.3H), 8.48 – 8.60 (m, 4.9H), 9.31 – 9.34 (m, 0.3H), 9.52 – 9.56 (m, 1H); ¹³C NMR (101 MHz, CDCl₃) δ 120.02, 121.77, 122.61, 123.07, 123.20, 123.26, 123.38, 123.64, 125.08, 125.31, 127.24, 127.62, 127.80, 127.95, 127.98, 128.25, 128.35, 128.40, 128.85, 128.93, 129.02, 129.05, 129.47, 129.49, 130.27, 130.29, 130.33, 131.09, 131.39, 131.45, 131.53, 132.48, 133.22, 134.77.

1.3. Synthesis of 7-bromobenzo[ghi]perylene (**S8**):

7-Bromobenzo[ghi]perylene **S8** (7-BrBGP) was synthesized from benzo[ghi]perylene **S7** (BGP) employing van Dijk's sodium metal reduction methodology² followed by bromination protocols as described.



Scheme 2. Synthesis of 7-bromobenzo[ghi]perylene **S8**.

7-Bromobenzo[ghi]perylene (S8). Freshly cut sodium metal (93 mg, 4.0 mmol) was added to a solution of **S7** (450 mg, 1.6 mmol) in THF (30 mL) at rt under Ar. After purging for 2 minutes, reaction was sonicated for 22 h and temperature maintained below 40 °C. Reaction color changed to deep purple and temperature was decreased to -78 °C. After 10 min, a solution of Br₂ (125 μL, 389 mg, 2.4 mmol) in THF (3 mL) was added and stirring was continued for 2.5 h. Reaction was quenched with sat. NH₄Cl and allowed to warm up to rt. Reaction mixture was partitioned between

dichloromethane and sat. NH_4Cl , washed with brine, and dried over Na_2SO_4 . Volatiles were evaporated and residue was column chromatographed (toluene/hexane; 100:0 \rightarrow 65:35) to provide **S8** (346 mg, 60%; 78% based on the recovered substrate **S7** (106 mg)) as a yellow solid: ^1H NMR (CDCl_3): δ 8.01 (t, $J = 7.8$ Hz, 1H), 8.09 (d, $J = 8.8$ Hz, 1H), 8.12 (d, $J = 8.8$ Hz, 1H), 8.19 (d, $J = 9.0$ Hz, 1H), 8.21 (d of br d, $J = 7.5, 0.8$ Hz, 1H), 8.23 (d, $J = 8.5$ Hz, 1H), 8.33 (d, $J = 8.2$ Hz, 1H), 8.36 (d, $J = 8.2$ Hz, 1H), 8.44 (d, $J = 9.1$ Hz, 1H), 8.77 (d, $J = 8.5$ Hz, 1H), 8.93 (d of br d, $J = 7.9, 0.6$ Hz, 1H); ^{13}C NMR δ 120.9, 121.4, 121.7, 123.7, 124.1, 125.5, 126.0, 126.1, 126.5, 126.6, 127.1, 127.2, 127.7, 127.8, 129.1, 129.3, 129.8, 130.0, 130.2, 130.5, 130.7, 132.3. HRMS (APPI-FTICR) calculated m/z for $\text{C}_{22}\text{H}_{11}\text{Br}$ $[\text{M}+\text{H}]^+$ 355.01169; observed m/z 355.01198.

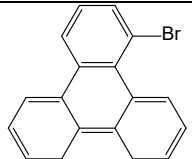
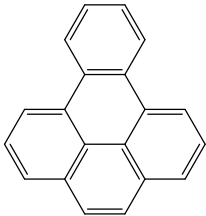
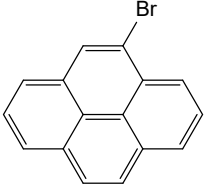
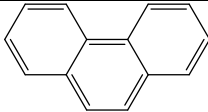
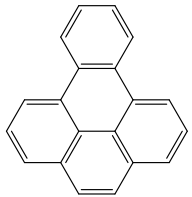
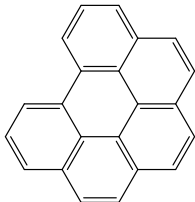
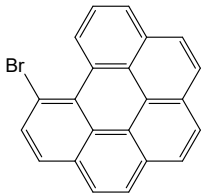
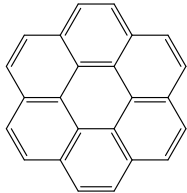
2. Mass Spectra Analysis

Additional signal that is only detectable with pyrolysis on occurs at $m/z = 226$ ($C_{18}H_{10}^+$), 227 ($^{13}CC_{17}H_{10}^+$, $C_{18}H_{11}^+$), 228 ($^{13}CC_{17}H_{11}^+$, $C_{18}H_{12}^+$), and 253 ($^{13}CC_{19}H_{12}^+$) (**1**), 200 ($C_{16}H_8^+$), 201 ($^{13}CC_{15}H_8^+$, $C_{16}H_9^+$), 202 ($^{13}CC_{15}H_9^+$, $C_{16}H_{10}^+$), 203 ($^{13}CC_{15}H_{10}^+$), 226 ($C_{18}H_{10}^+$), 227 ($^{13}CC_{17}H_{10}^+$), and 253 ($^{13}CC_{19}H_{12}^+$) (**2**), 254 ($C_{20}H_{14}^+$) and 255 ($^{13}CC_{19}H_{14}^+$) (**3**), and 275 ($C_{22}H_{11}^+$), 276 ($^{13}CC_{21}H_{11}^+$, $C_{22}H_{12}^+$), 277 ($^{13}CC_{21}H_{12}^+$), 301 ($^{13}CC_{23}H_{12}^+$), and 324 ($C_{26}H_{12}^+$) (**4**). For reaction (**1**), signal at $m/z = 227$ can be attributed to the 1-triphenylenyl radical ($C_{18}H_{11}^{\bullet}$) formed via bromine loss from the 1-bromotriphenylene ($C_{18}H_{11}Br$) precursor. Ions at $m/z = 226$ may occur from subsequent hydrogen atom abstraction from 1-triphenylenyl forming 1,2-didehydrotriphenylene ($C_{18}H_{10}$), while ions at $m/z = 228$ are from recombination of the 1-triphenylenyl radical with atomic hydrogen forming triphenylene ($C_{18}H_{12}$). Counts at $m/z = 253$ arise from ^{13}C -substituted benzo[*e*]pyrene ($C_{20}H_{12}$). For reaction (**2**), signal at $m/z = 201$ may correspond to the 4-pyrenyl radical ($C_{16}H_9^{\bullet}$) formed by bromine loss from 4-bromopyrene ($C_{16}H_9Br$). Ions at $m/z = 200$ likely arise from subsequent H atom abstraction from 4-pyrenyl forming 4,5-didehydropyrene ($C_{16}H_8$), while ions at $m/z = 202$ and 203 are from recombination of the 4-pyrenyl radical with atomic hydrogen forming pyrene ($C_{16}H_{10}$) as well as ^{13}C -pyrene ($^{13}CC_{15}H_{10}$), respectively. Counts at $m/z = 226$ and 227 occur from the reaction of 4-pyrenyl radicals with acetylene (a minor impurity from the vinylacetylene cylinder), producing 4-ethynylpyrene ($C_{18}H_{10}$) and ^{13}C -4-ethynylpyrene ($^{13}CC_{17}H_{10}$). ^{13}C -substituted benzo[*e*]pyrene is also found at $m/z = 253$. For reaction (**3**), peaks at $m/z = 254$ and 255 are due to phenylphenanthrene ($C_{20}H_{14}$) and ^{13}C -phenylphenanthrene ($^{13}CC_{19}H_{14}$) isomer(s) formed from phenyl addition to phenanthrene but without subsequent dehydrocyclization. For reaction (**4**), peaks at $m/z = 275$, 276, and 277 are due to 7-benzo[*ghi*]perylene radicals ($C_{22}H_{11}^{\bullet}$) from bromine loss of 7-bromobenzo[*ghi*]perylene ($C_{22}H_{11}Br$), benzo[*ghi*]perylene ($C_{22}H_{12}$) from subsequent recombination with a hydrogen atom, and ^{13}C -benzo[*ghi*]perylene ($^{13}CC_{21}H_{12}$). The peak at $m/z = 301$ is due to ^{13}C -substituted coronene ($^{13}CC_{23}H_{12}$), and the peak at $m/z = 324$ can be attributed to H atom abstraction from coronene followed by addition to a second acetylene molecule forming ethynylcoronene ($C_{26}H_{12}$). The photoionization efficiency (PIE) curves of all species shown in the mass spectra (Figure 4), aside from those in Figures 5–7, are shown in Figures S1–S4, and mass-selected threshold photoelectron (ms-TPE) spectra for $m/z = 226$ (**1**) and 254 (**3**) are shown in Figures S5 and S6.

3. Test Reaction

A test reaction of the previously studied system³ of phenyl radicals ($C_6H_5^{\bullet}$) with acetylene (C_2H_2) was conducted to verify the operating conditions of the experimental setup. Briefly, nitrosobenzene (C_6H_5NO , 97%, Sigma-Aldrich) was seeded at a level of a few tenths of a percent in acetylene (C_2H_2 , $\geq 99.5\%$; PANGAS; acetone traces removed via ethanol/dry ice bath) set to a backing pressure of 270 Torr. The gas mixture was introduced through a 0.1 mm nozzle to the SiC microreactor, which had a 1 mm inner diameter and heated length of 12 mm kept at 900 ± 100 K. Products formed attained supersonic expansion upon exiting the reactor and passed through a 2 mm diameter skimmer into the spectrometer chamber where they were photoionized by vacuum ultraviolet (VUV) light at photon energies from 8–9 eV. Photoions and photoelectrons are extracted by a constant electric field of 218 V cm^{-1} and collected in coincidence via VMI on two position-sensitive delay-line anode detectors (Roentdek DLD40). Photoionization efficiency (PIE) curves and mass-selected threshold photoelectron (ms-TPE) spectra were obtained at mass-to-charge ratios (m/z) of 102 ($C_8H_6^+$) (Figure S7) and 128 ($C_{10}H_8^+$) (Figure S8) and are compared to reference spectra. At $m/z = 102$, the experimental PIE curve (Figure S7a) features an ionization onset of 8.80 ± 0.05 eV which matches the phenylacetylene reference onset of 8.80 ± 0.05 eV from Parker et al.³ while the curve shapes also overlap nicely. The experimental ms-TPES (Figure S7b) has three strong peaks at 8.84, 8.88, and 8.98 ± 0.05 eV which are matched by the reference spectrum from West et al.⁴ Similarly, the experimental $m/z = 128$ PIE (Figure S8a) and ms-TPES (Figure S8b) feature strong overlap with the naphthalene reference curves from Parker et al.³ and Rühl et al.,⁵ respectively. Briefly, the experimental and reference PIEs both exhibit ionization onsets of about 8.10 ± 0.05 eV and match fairly well over the scanned range of 8–9 eV. The experimental ms-TPES contains six peaks at 8.16, 8.24, 8.28, 8.34, 8.46, and 8.52 ± 0.05 eV, which match quite well with the naphthalene reference curve. Each peak can be assigned to the fundamental (0_0^0), skeletal longitudinal stretching (9_0^1), skeletal breathing (7_0^1), C–C in-plane transannular stretching (4_0^1), combination ($4_0^1 7_0^1$), and overtone (4_0^2) vibronic transitions, respectively, using values from Behlen and Rice⁶ and from Cockett et al.⁷

Table S1. Experimental conditions for reactions (1)–(5).

	Reactant 1	Precursor 2	Comment Reactant 1	Comment Precursor 2	Product
(1)	C ₂ H ₂	 1-Bromotriphenylene	Gas 75 Torr	T(oven) = 423 K T(SiC) = 1300 K	 Benzo[<i>e</i>]pyrene
(2)	C ₄ H ₄ (5 % in He)	 4-Bromopyrene	Gas 75 Torr	T(oven) = 403 K T(SiC) = 1400 K	
(3)	C ₆ H ₅ NO (1 % in He)	 Phenanthrene	T(Bub) = 293 K 90 Torr	T(oven) = 358 K T(SiC) = 1300 K	
(4)	C ₂ H ₂	 Benzo[<i>e</i>]pyrene	Gas 75 Torr	T(oven) = 423 K T(SiC) = 1300 K	 Benzo[<i>ghi</i>]perylene
(5)	C ₂ H ₂	 7-Bromobenzo[<i>ghi</i>]perylene	Gas 165 Torr	T(oven) = 358 K T(SiC) = 1500 K	 Coronene

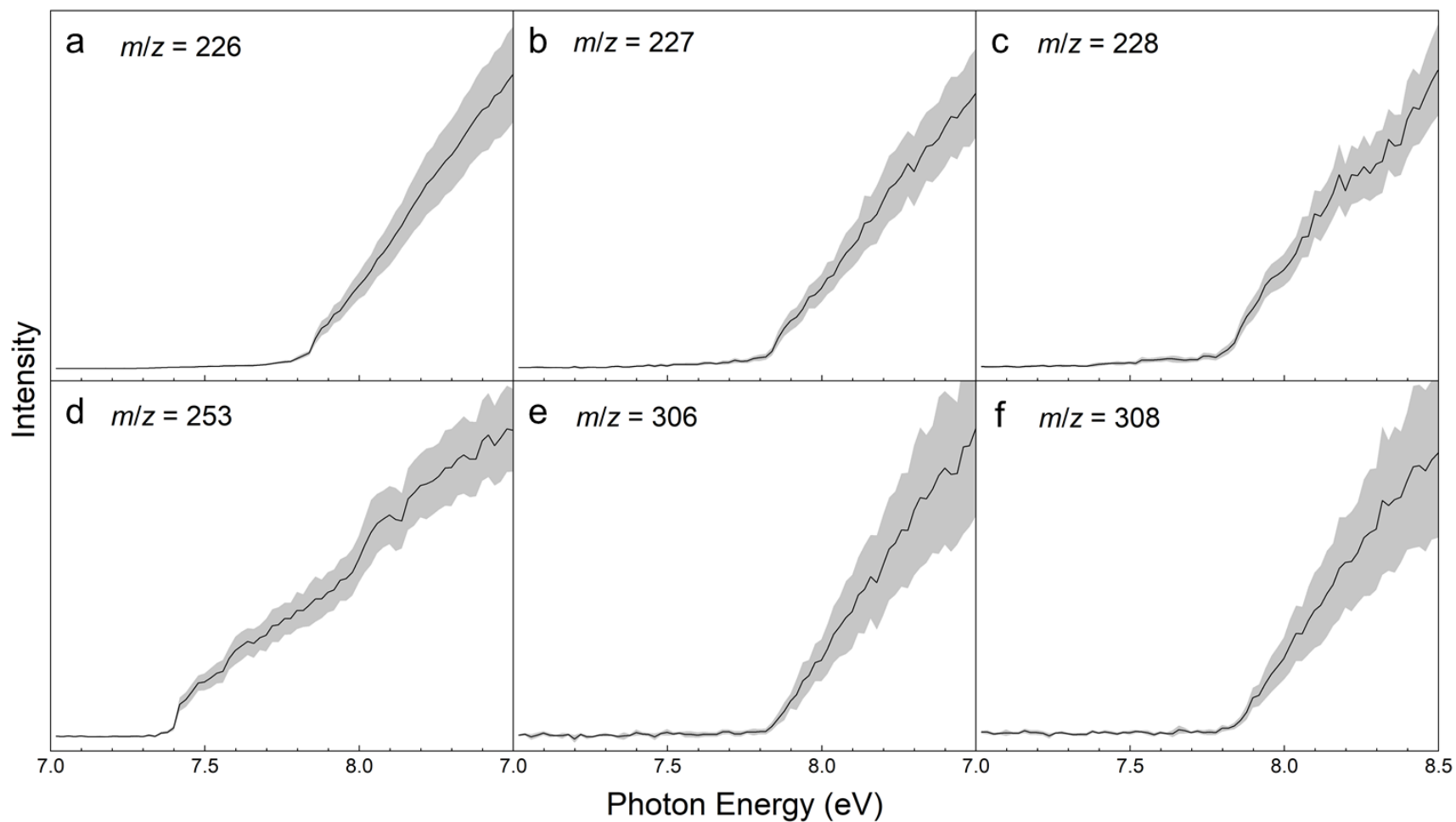


Figure S1. Photoionization efficiency (PIE) curves for the acetylene (C_2H_2) – 1-bromotriphenylene ($C_{18}H_{11}Br$) system at (a) $m/z = 226$ ($C_{18}H_{10}$), (b) $m/z = 227$ ($C_{18}H_{11}$), (c) $m/z = 228$ ($C_{18}H_{12}$), (d) $m/z = 253$ ($^{13}CC_{19}H_{12}$), (e) $m/z = 306$ ($C_{18}H_{11}^{79}Br$), and (f) $m/z = 308$ ($C_{18}H_{11}^{81}Br$). The overall error bars (gray area) consist of two parts: 1σ error of the PIE curve averaged over the individual scans and $\pm 10\%$ based on the accuracy of the photodiode.

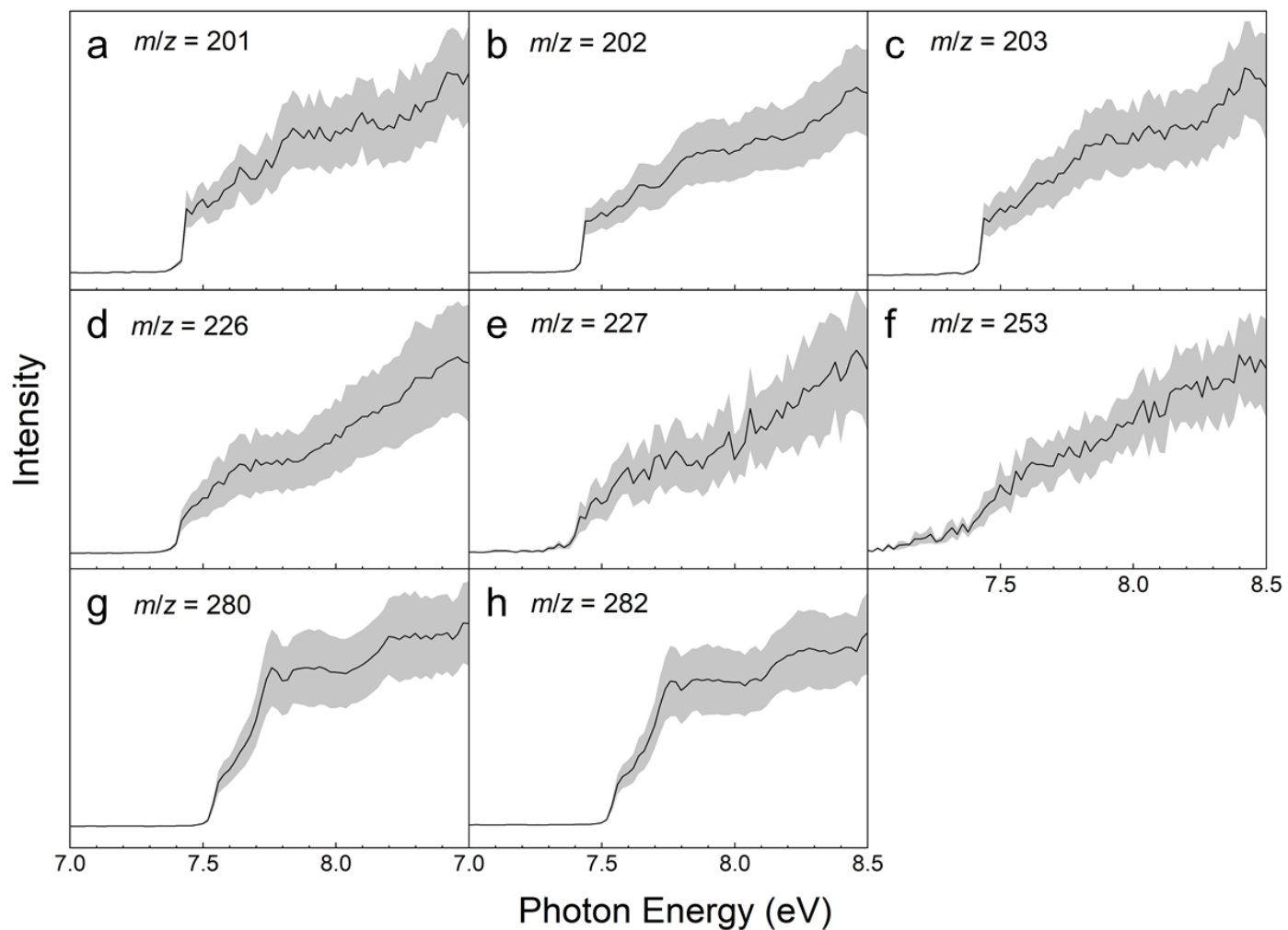


Figure S2. Photoionization efficiency (PIE) curves for the vinylacetylene (C_4H_4) – 4-bromopyrene ($C_{16}H_9Br$) system at (a) $m/z = 201$ ($C_{16}H_9$), (b) $m/z = 202$ ($C_{16}H_{10}$), (c) $m/z = 203$ ($^{13}CC_{15}H_{10}$), (d) $m/z = 226$ ($C_{18}H_{10}$), (e) $m/z = 227$ ($^{13}CC_{17}H_{10}$), (f) $m/z = 253$ ($^{13}CC_{19}H_{12}$), (g) $m/z = 280$ ($C_{16}H_9^{79}Br$), and (h) $m/z = 282$ ($C_{16}H_9^{81}Br$). The overall error bars (gray area) consist of two parts: 1σ error of the PIE curve averaged over the individual scans and $\pm 10\%$ based on the accuracy of the photodiode.

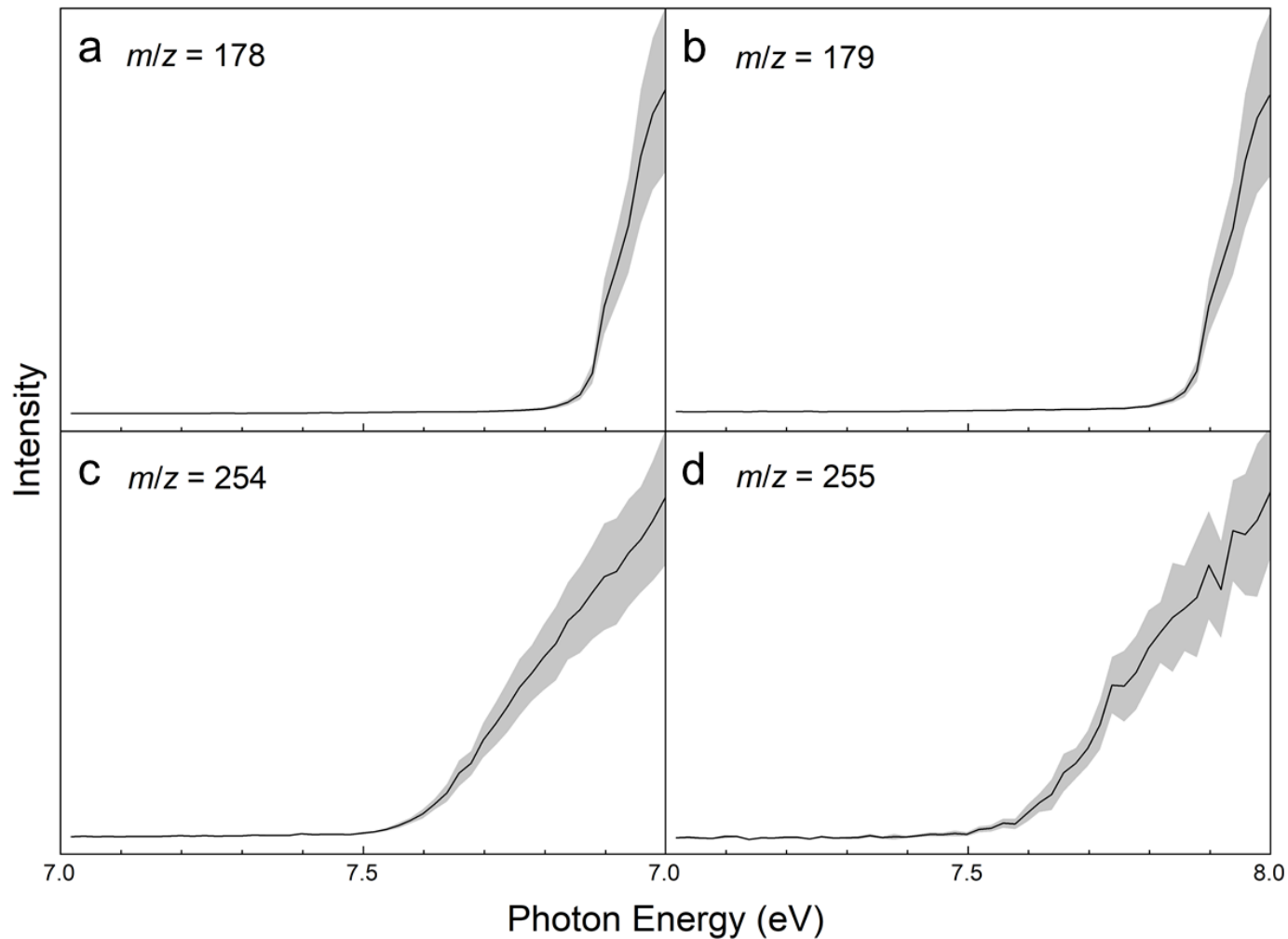


Figure S3. Photoionization efficiency (PIE) curves for the nitrosobenzene (C_6H_5NO) – phenanthrene ($C_{14}H_{10}$) system at (a) $m/z = 178$ ($C_{14}H_{10}$), (b) $m/z = 179$ ($^{13}CC_{13}H_{10}$), (c) $m/z = 254$ ($C_{20}H_{14}$), and (d) $m/z = 255$ ($^{13}CC_{19}H_{14}$). The overall error bars (gray area) consist of two parts: 1σ error of the PIE curve averaged over the individual scans and $\pm 10\%$ based on the accuracy of the photodiode.

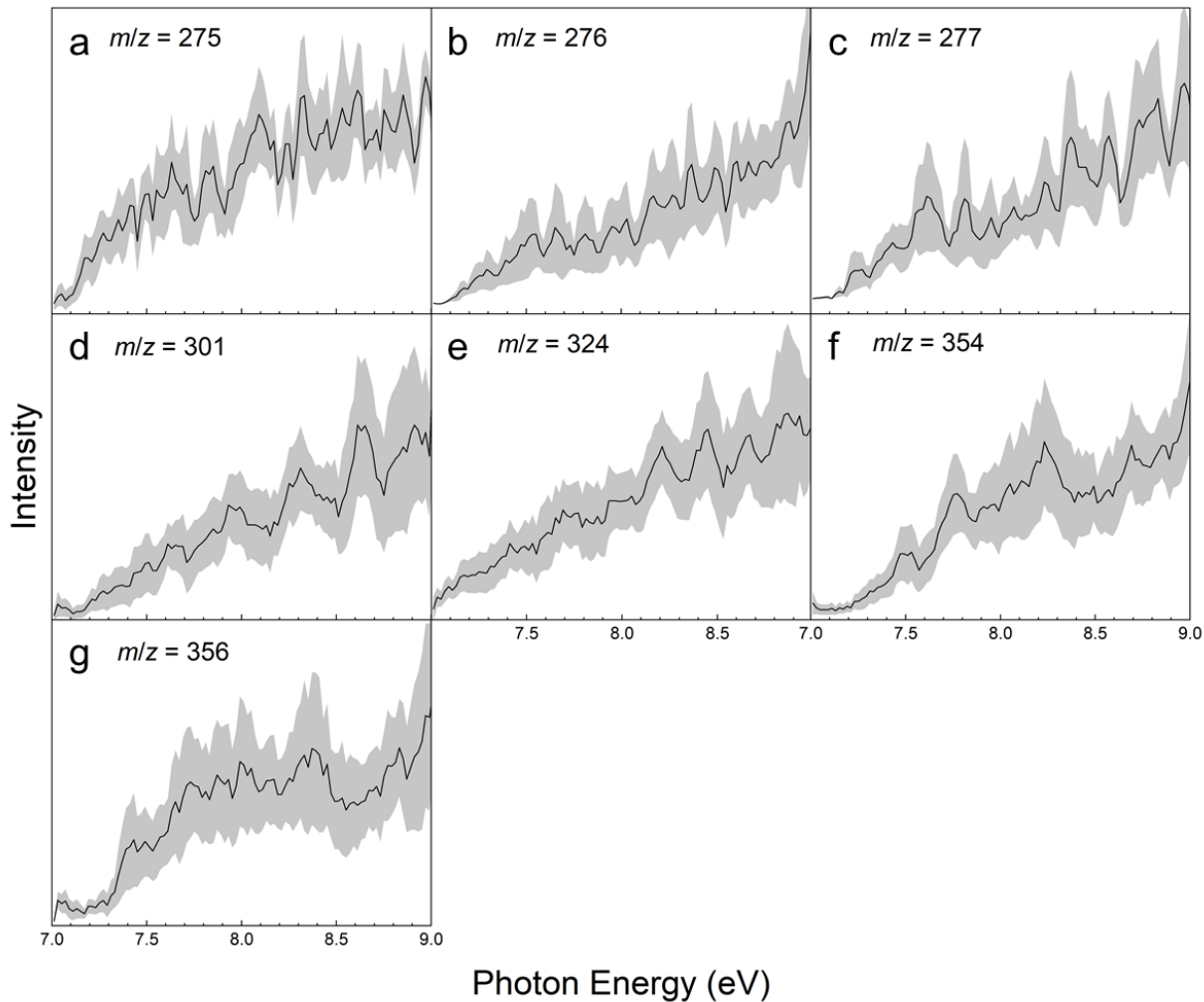


Figure S4. Photoionization efficiency (PIE) curves for the acetylene (C_2H_2) – 7-bromobenzo[*ghi*]perylene ($C_{22}H_{11}Br$) system at (a) $m/z = 275$ ($C_{22}H_{11}$), (b) $m/z = 276$ ($C_{22}H_{12}$), (c) $m/z = 277$ ($^{13}CC_{21}H_{12}$), (d) $m/z = 301$ ($^{13}CC_{24}H_{12}$), (e) $m/z = 324$ ($C_{26}H_{12}$), (f) $m/z = 354$ ($C_{22}H_{11}^{79}Br$), and (g) $m/z = 356$ ($C_{22}H_{11}^{81}Br$). The overall error bars (gray area) consist of two parts: 1σ error of the PIE curve averaged over the individual scans and $\pm 10\%$ based on the accuracy of the photodiode.

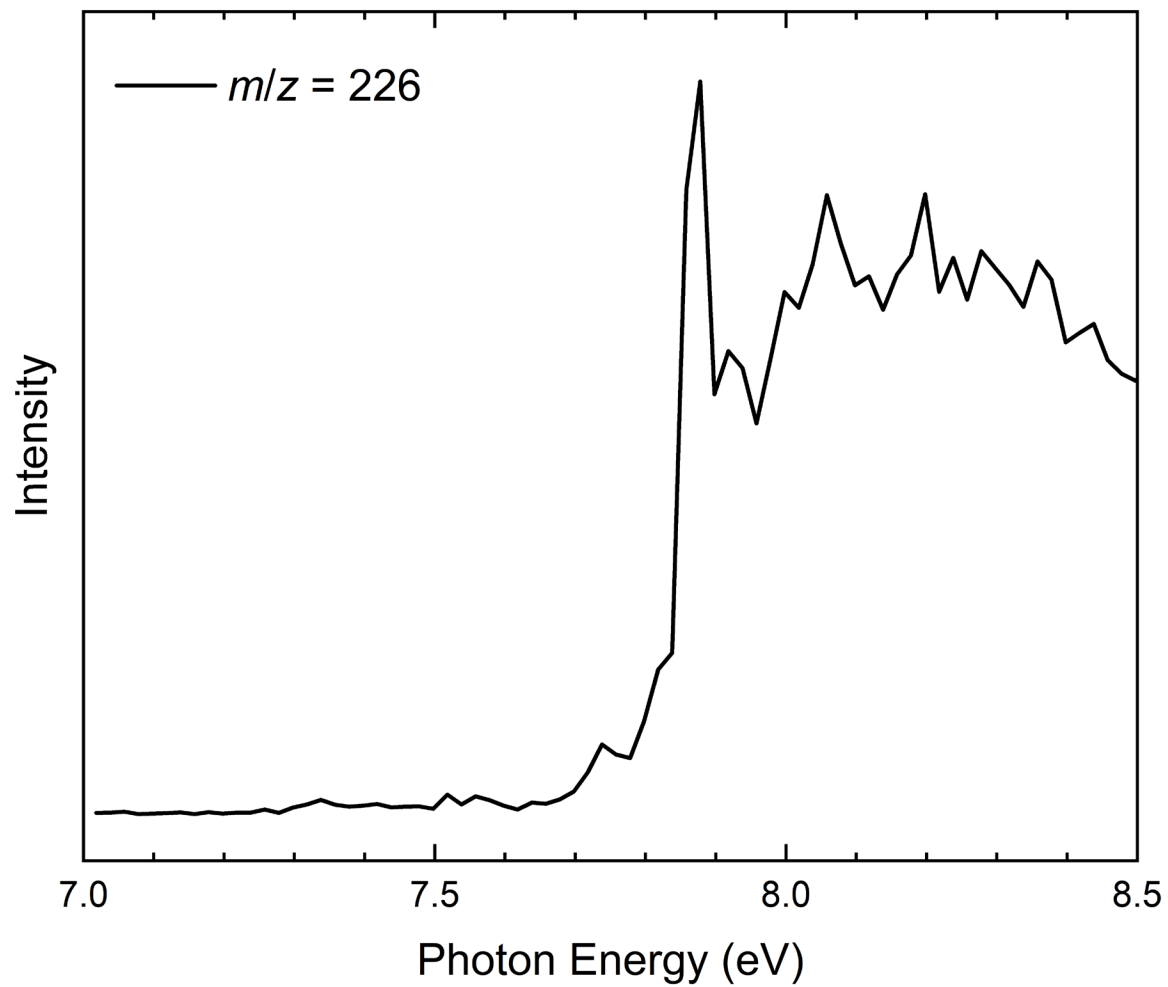


Figure S5. Mass-selected threshold photoelectron (ms-TPE) spectrum for the acetylene (C_2H_2) – 1-bromotriphenylene ($C_{18}H_{11}Br$) system at $m/z = 226$.

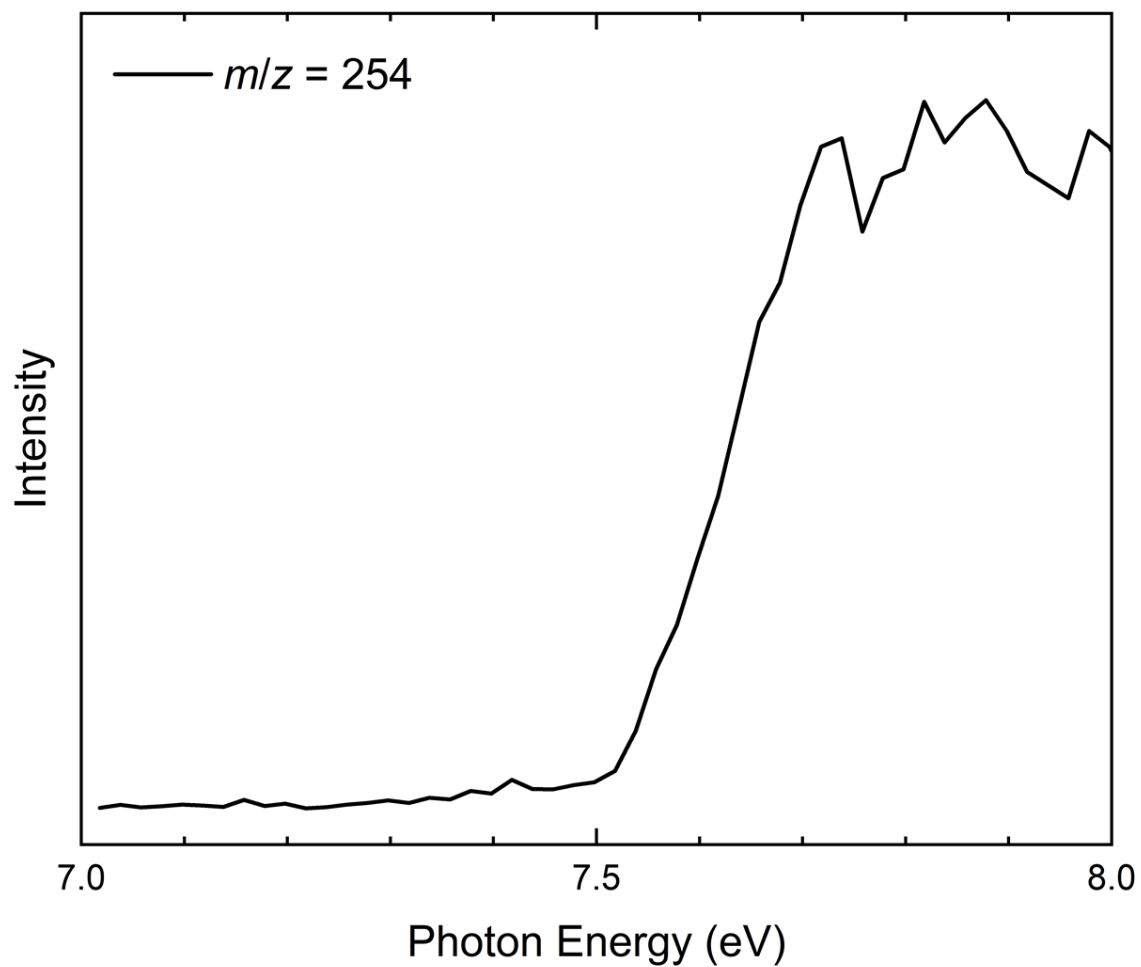


Figure S6. Mass-selected threshold photoelectron (ms-TPE) spectrum for the nitrosobenzene (C_6H_5NO) – phenanthrene ($C_{14}H_{10}$) system at $m/z = 254$.

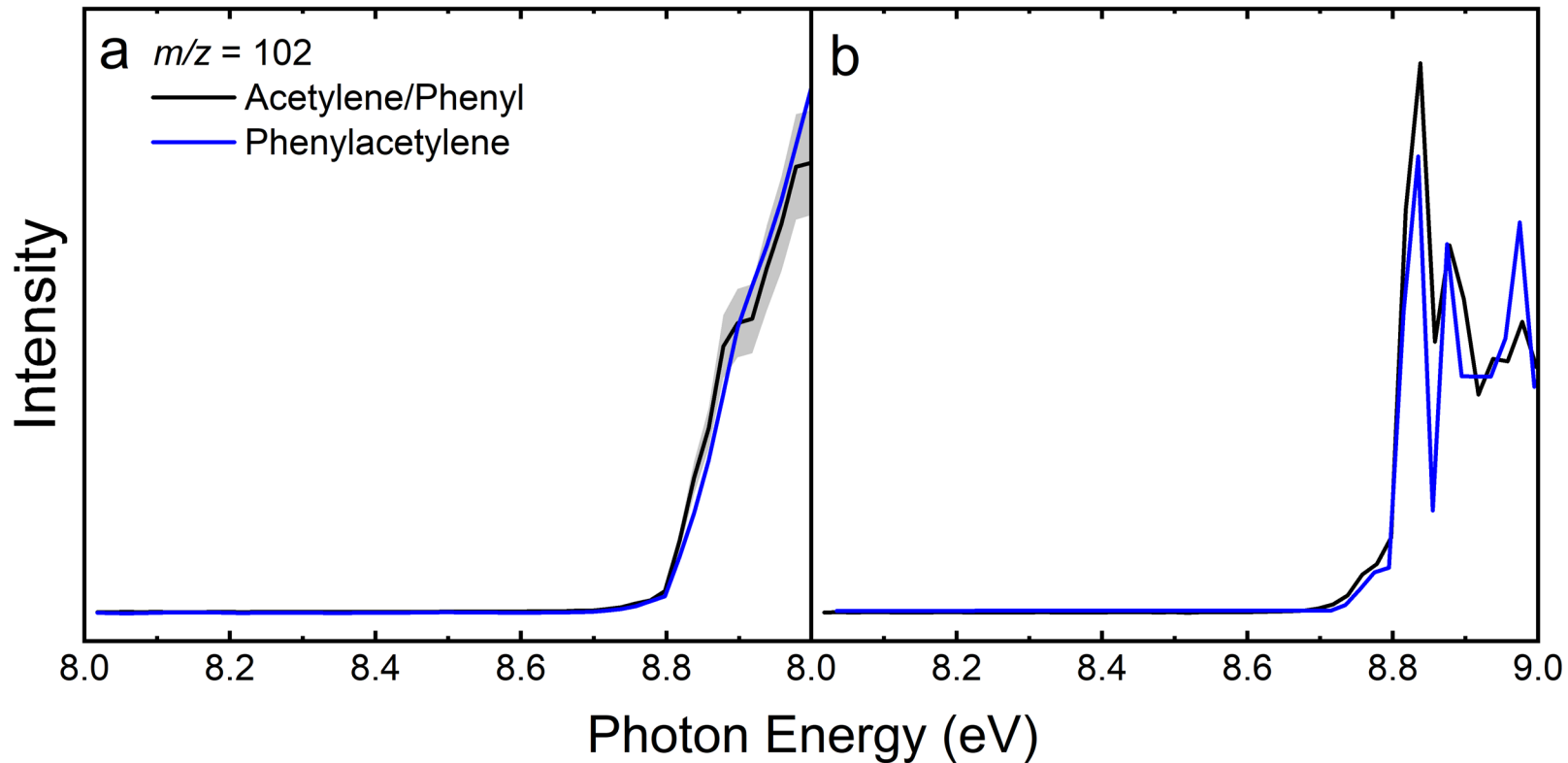


Figure S7. Photoionization efficiency (PIE) curves (**a**) and mass-selected threshold photoelectron (ms-TPE) spectra (**b**) for the acetylene (C_2H_2) – phenyl ($C_6H_5^+$) test reaction at $m/z = 102$. Black: experimental curves; blue: phenylacetylene reference curves obtained from Parker et al.³ and West et al.⁴ The overall error bars (gray area) consist of two parts: 1σ error of the PIE curve averaged over the individual scans and $\pm 10\%$ based on the accuracy of the photodiode.

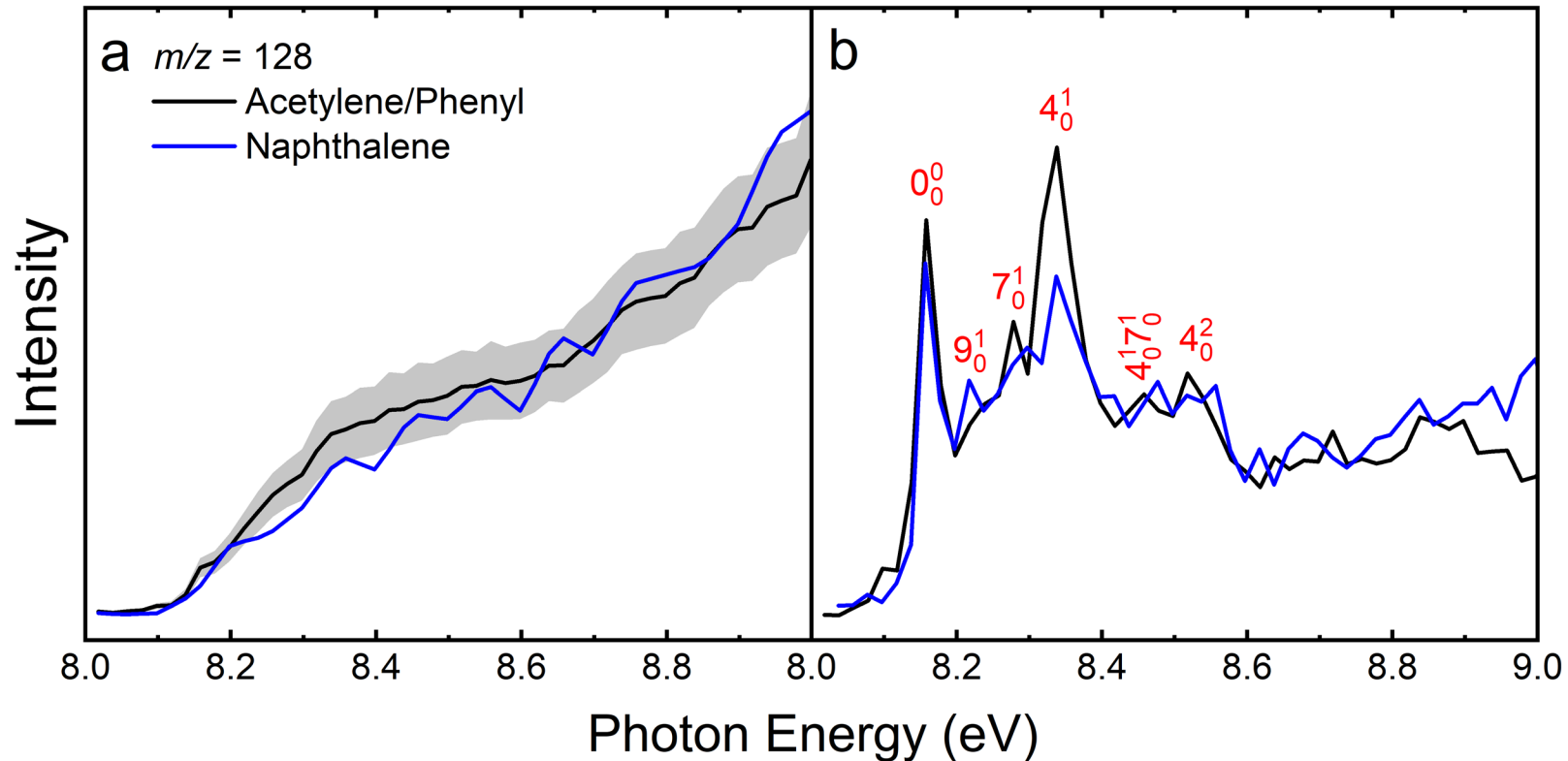


Figure S8. Photoionization efficiency (PIE) curves (**a**) and mass-selected threshold photoelectron (ms-TPE) spectra (**b**) for the acetylene (C_2H_2) – phenyl ($C_6H_5^+$) test reaction at $m/z = 128$. Black: experimental curves; blue: naphthalene reference curves obtained from Parker et al.³ and Rühl et al.⁵ Vibronic transition assignments were made using values from Behlen and Rice⁶ and from Cockett et al.⁷ The overall error bars (gray area) consist of two parts: 1σ error of the PIE curve averaged over the individual scans and $\pm 10\%$ based on the accuracy of the photodiode.

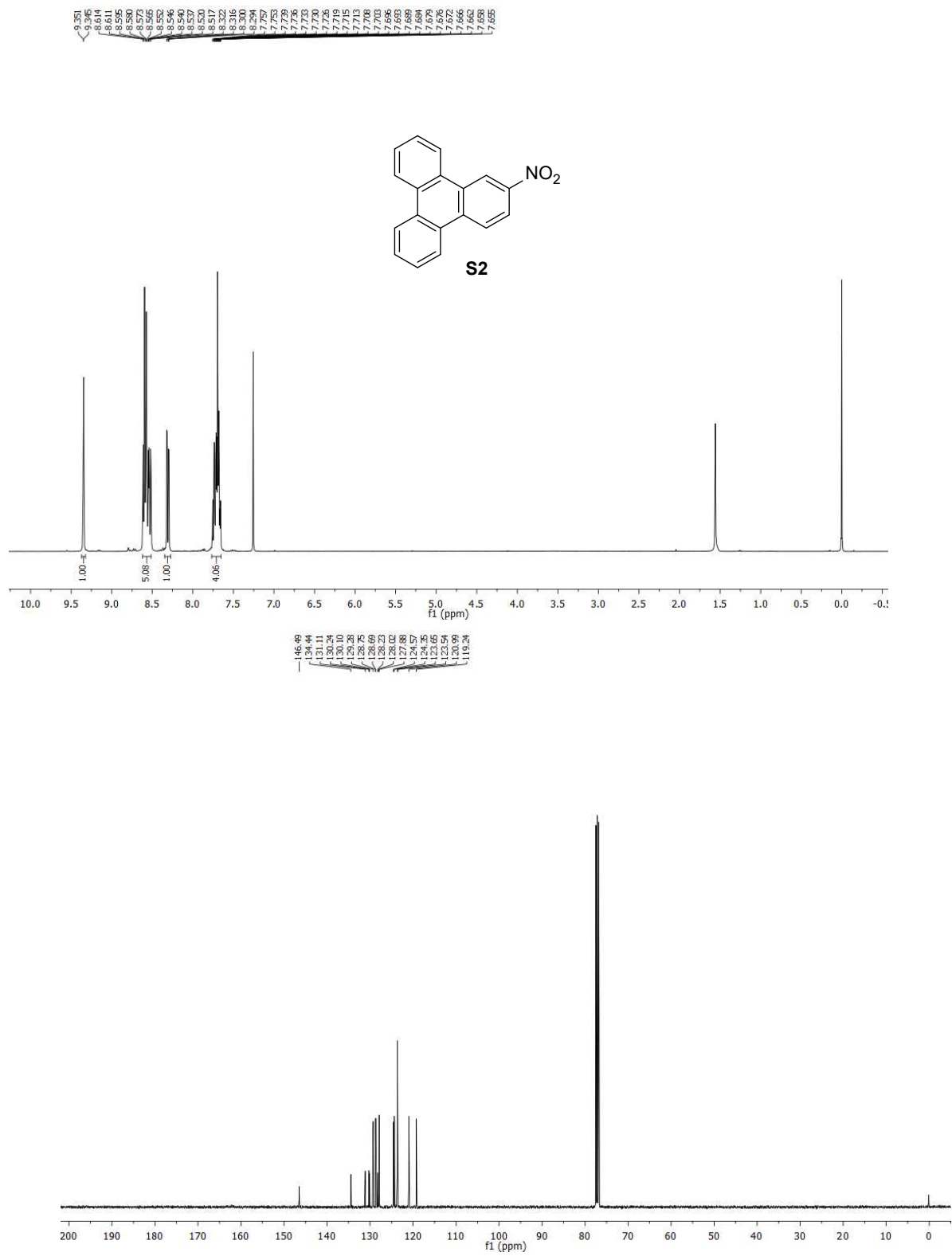


Figure S9. ¹H NMR and ¹³C NMR spectra of compound **S2** in CDCl₃

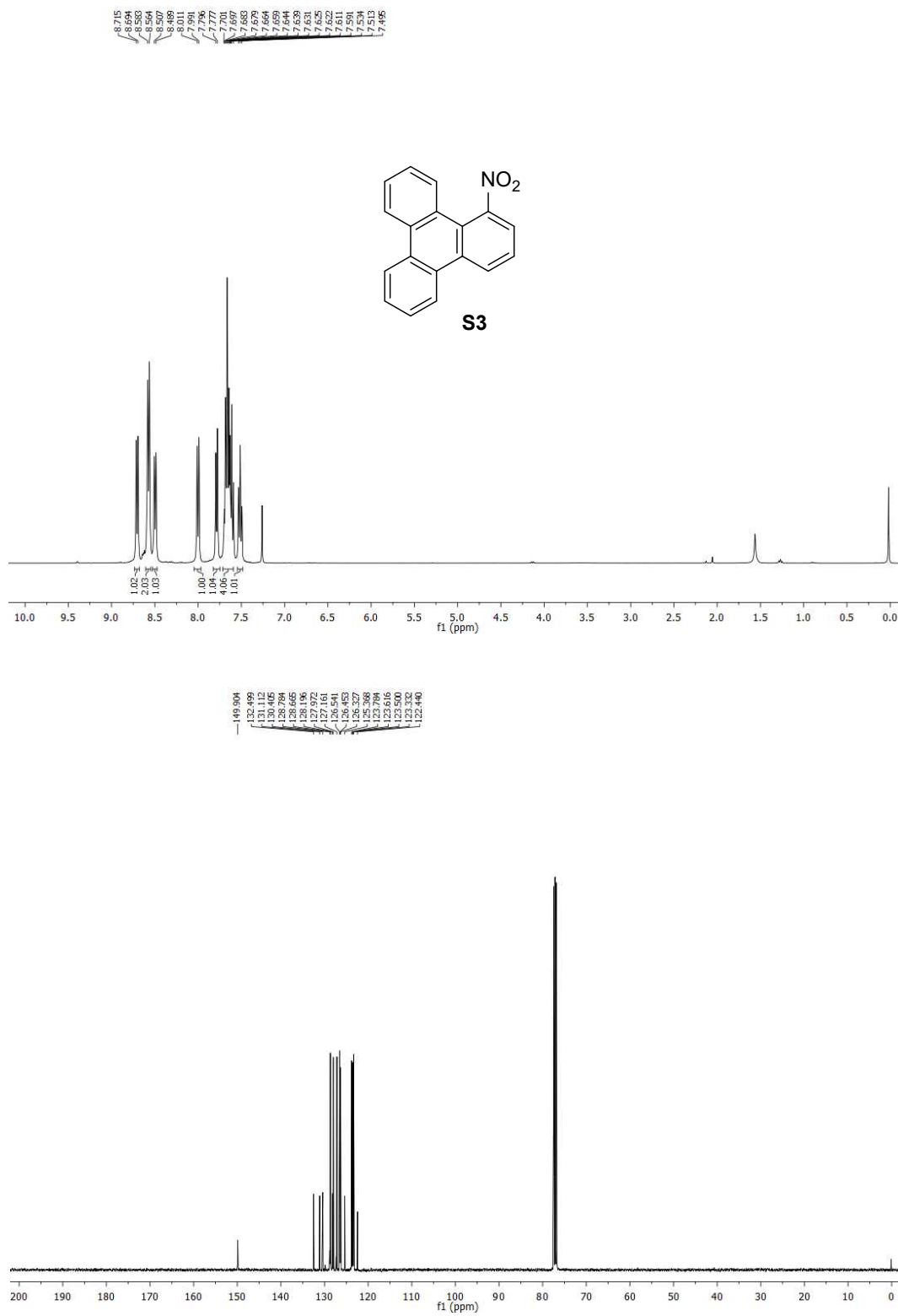


Figure S10. ¹H NMR and ¹³C NMR spectra of compound **S3** in CDCl₃.

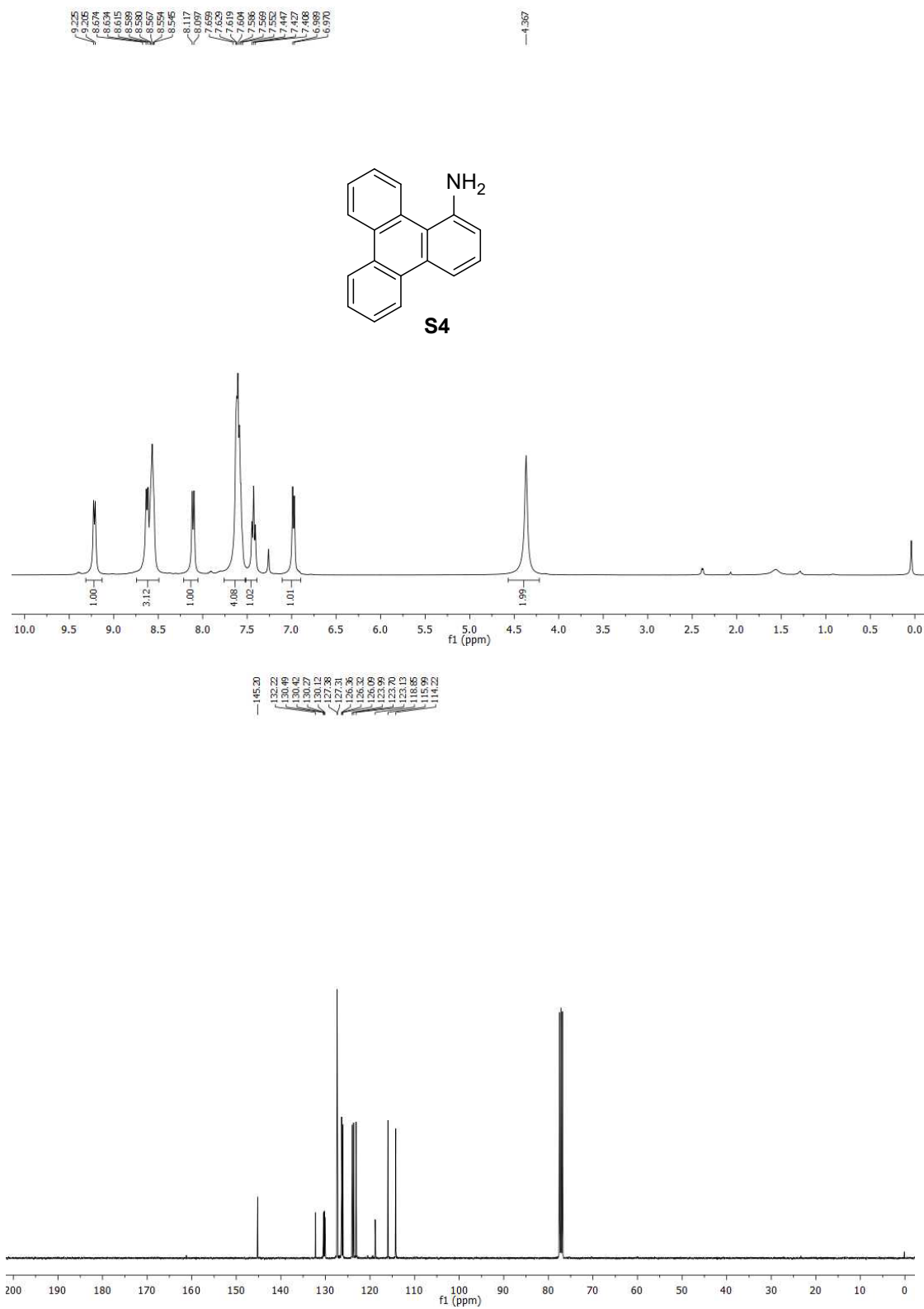


Figure S11. ¹H NMR and ¹³C NMR spectra of compound **S4** in CDCl₃.

Supporting References

- (1) Barker, C. C.; Emmerson, R. G.; Periam, J. D. The monosubstitution of triphenylene. *J. Chem. Soc.* **1955**, 4482.
- (2) van Dijk, J. T. M.; Hartwijk, A.; Bleeker, A. C.; Lugtenburg, J.; Cornelisse, J. Gram scale synthesis of benzo[ghi]perylene and coronene. *J. Org. Chem.* **1996**, *61*, 1136.
- (3) Parker, D. S.; Kaiser, R. I.; Troy, T. P.; Ahmed, M. Hydrogen abstraction/acetylene addition revealed. *Angew. Chem., Int. Ed.* **2014**, *53*, 7740.
- (4) West, B.; Sit, A.; Bodi, A.; Hemberger, P.; Mayer, P. M. Dissociative photoionization and threshold photoelectron spectra of polycyclic aromatic hydrocarbon fragments: An imaging photoelectron photoion coincidence (iPEPICO) study of four substituted benzene radical cations. *J. Phys. Chem. A* **2014**, *118*, 11226.
- (5) Rühl, E.; Price, S. D.; Leach, S. Single and double photoionization processes in naphthalene between 8 and 35 eV. *J. Phys. Chem.* **1989**, *93*, 6312.
- (6) Behlen, F. M.; Rice, S. A. Intersystem crossing in cold isolated molecules of naphthalene. *J. Chem. Phys.* **1981**, *75*, 5672.
- (7) Cockett, M. C. R.; Ozeki, H.; Okuyama, K.; Kimura, K. Vibronic coupling in the ground cationic state of naphthalene: A laser threshold photoelectron [zero kinetic energy (ZEKE)-photoelectron] spectroscopic study. *J. Chem. Phys.* **1993**, *98*, 7763.